SUPPORTING INFORMATION

Electrochemical Control Over Stoichiometry via Cation Intercalation into Chevrel Phase Sulphides ($Cu_xMo_6S_8$, x = 1-3)

Kabian A. Ritter,[a,b] Konstantina G. Mason,[a] Suxuen Yew,[d] Joseph T. Perryman,[c] Jessica C. Ortiz-Rodríguez,[a] Nicholas R. Singstock,*[d] Brian A. Wuille Bille,*[a] Charles B. Musgrave,[d] Jesús M. Velázquez,*[a,b]

[a.] *Department of Chemistry, University of California, One Shields Avenue, Davis, California 95616, USA. E-mail: jevelazquez@ucdavis.edu.*
[b.] *Energy Systems, Energy and Efficiency Institute, University of California, 1605 Tilia St #100, Davis, California 95616, USA.*
[c.] *Department of Chemical Engineering, Stanford University, 381 North-South Mall, Stauffer II, Stanford, California 94305, USA.*
[d.] *Department of Chemical and Biological Engineering, University of Colorado Boulder, Boulder, Colorado 80303, United States; Email:*
** Corresponding author.*

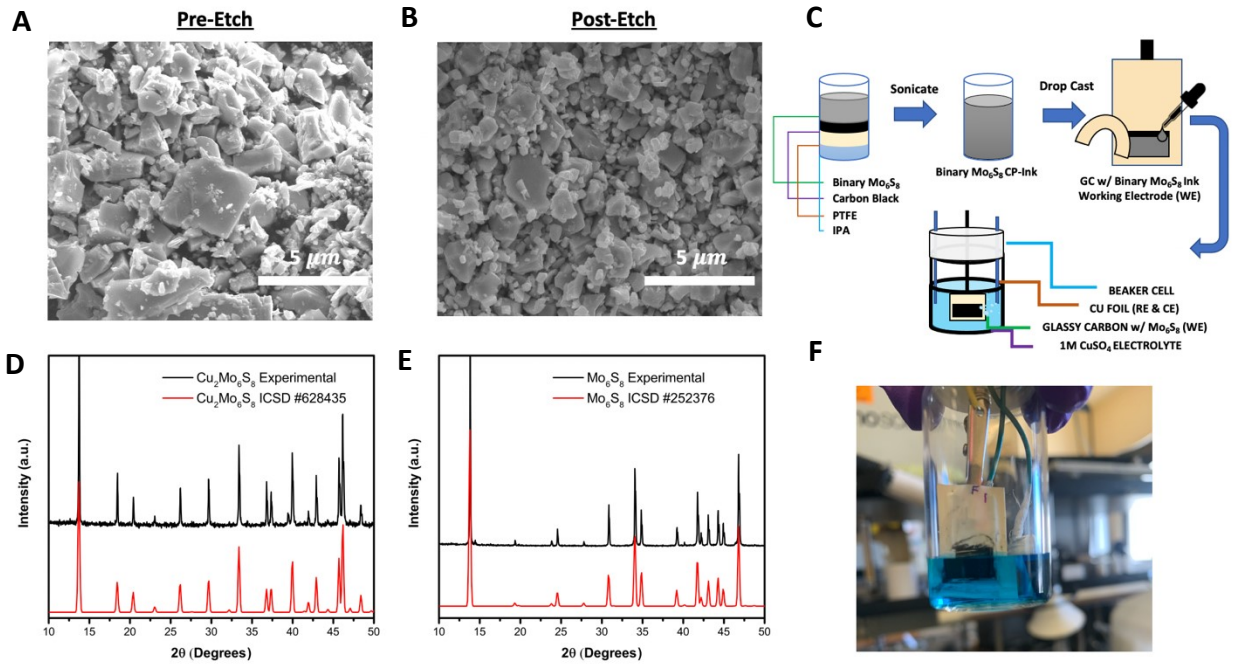

Figure S1. SEM images of microwave-assisted solid-state synthesized $Cu_2Mo_6S_8$ (A) and post-acid etch SEM showing the resulting binary Mo_6S_8. A schematic of the ink making process and working electrode configuration (C). Complementary PXRD data with the corresponding reference pattern confirming the purity of the synthesized $Cu_2Mo_6S_8$ (D) binary Mo_6S_8. (E). Schematic of ink making process, working electrode configuration, and an image showing the experimental setup (F).

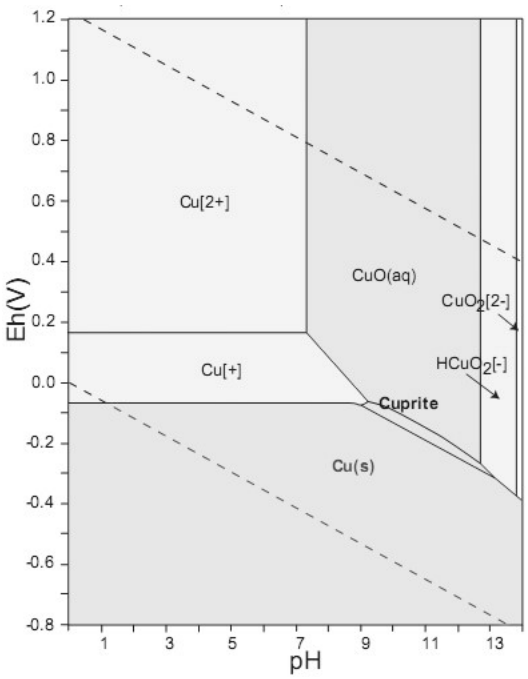

Figure S2. Pourbaix diagram at 25 °C, 1 atm, and 10 mM Cu concentration in aqueous media, reproduced from ref. [1] with permission from Elsevier.

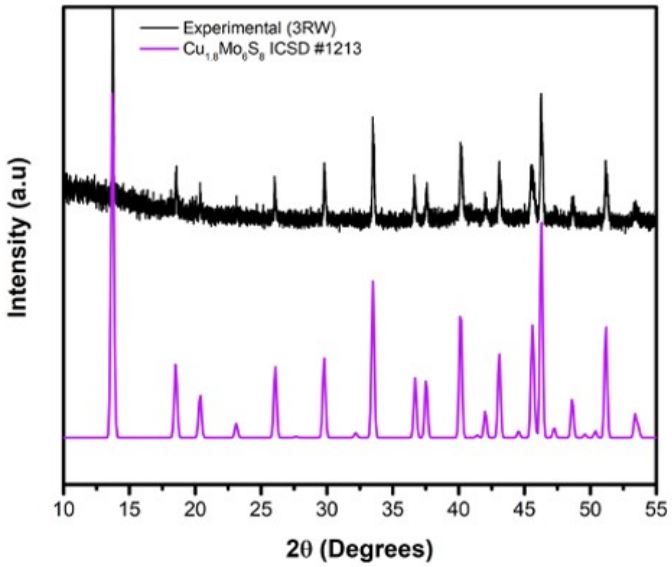

Figure S3. Non-stoichiometric phase, $Cu_{1.8}Mo_6S_8$, achieved at 0.17 V during electrochemical intercalation in aqueous 1M $CuSO_4$

Table S1. Lattice parameters extracted from Rietveld Refinement of $Cu_1Mo_6S_8$, $Cu_2Mo_6S_8$, and $Cu_3Mo_6S_8$ experimental XRD patterns.

Sample	a (Å)	C (Å)	Vol. $(Å)^3$
$CuMo_6S_8$	9.42082	10.41312	800.367
$Cu_2Mo_6S_8$	9.61968	10.20789	818.065
$Cu_3Mo_6S_8$	9.70260	10.22275	833.440

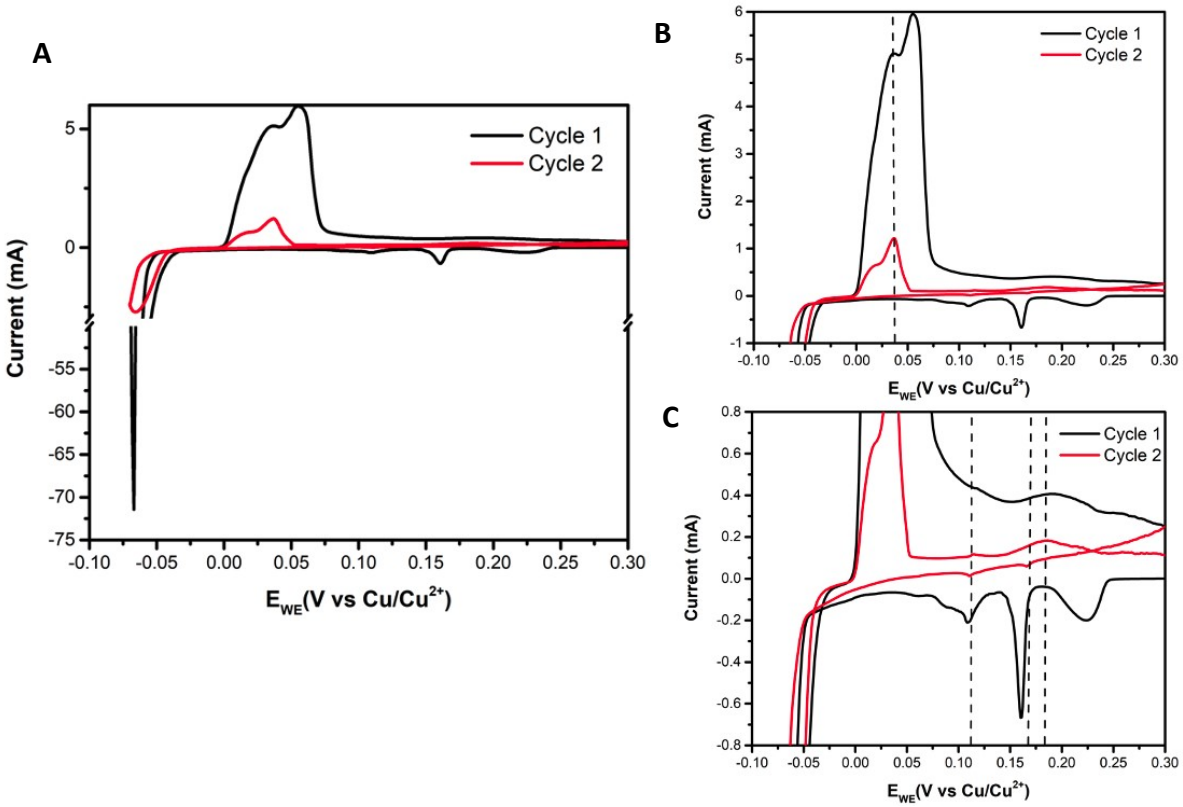

Figure S4. (A) CV extending to -0.07V vs Cu/Cu^{2+} with displayed nucleation loop indicative of intercalation and co-plating. Magnified view of the CV (B) and LSV (C) showing the current response peaks are preserved. Dashed lines in (B) and (C) are to guide the reader on the shift in potential between cycles 1 and 2.

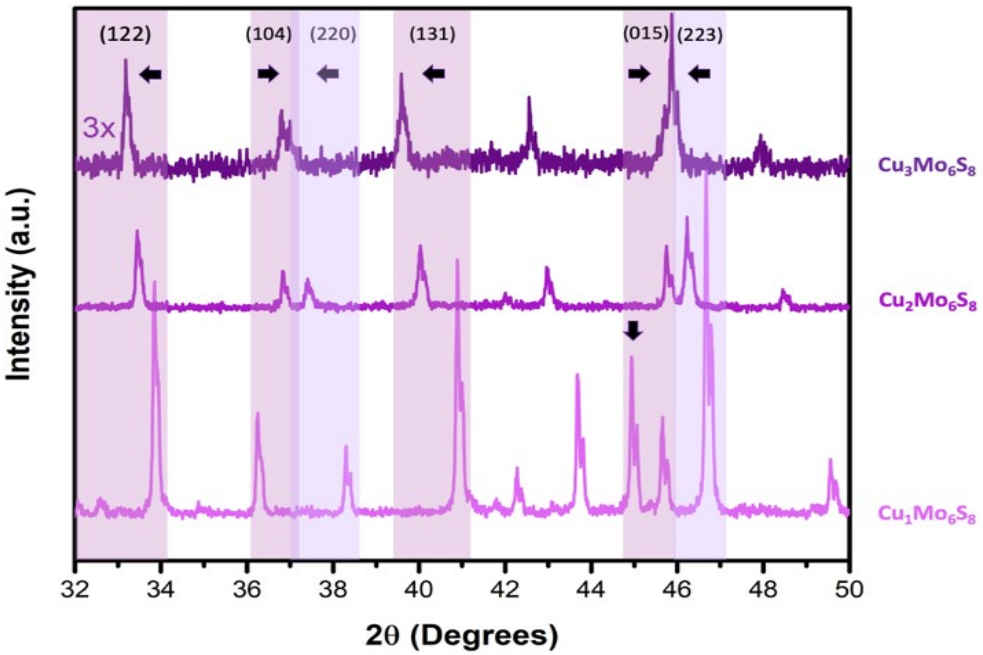

Figure S5. Powder X-ray diffractograms for $Cu_1Mo_6S_8$, $Cu_2Mo_6S_8$, and $Cu_3Mo_6S_8$ highlighting relevant crystallographic planes and their progressive shift as intercalation progresses. Overlapping regions describe a merging of peaks depicting overlap in the reflections of these crystal planes. An orienting arrow is drawn above the (015) peak in $Cu_1Mo_6S_8$ to differentiate between (015), left, and the (223), right reflections.

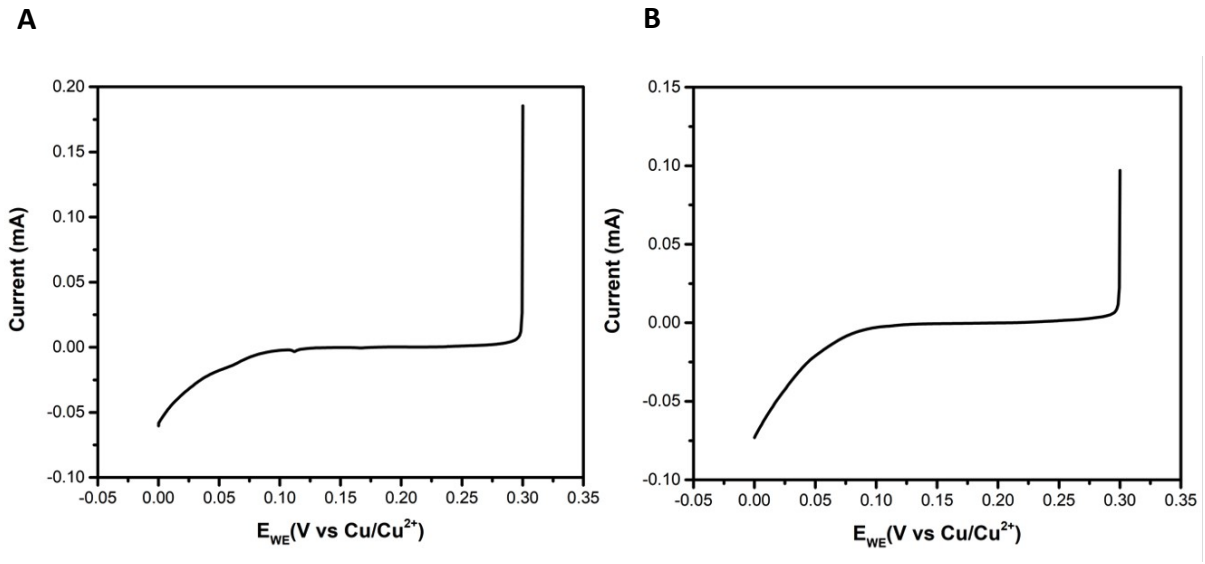

Figure S6. Background LSV scans of (A) a bare glassy carbon electrode and (B) Ink without the Chevrel phase deposited on a glassy carbon electrode.

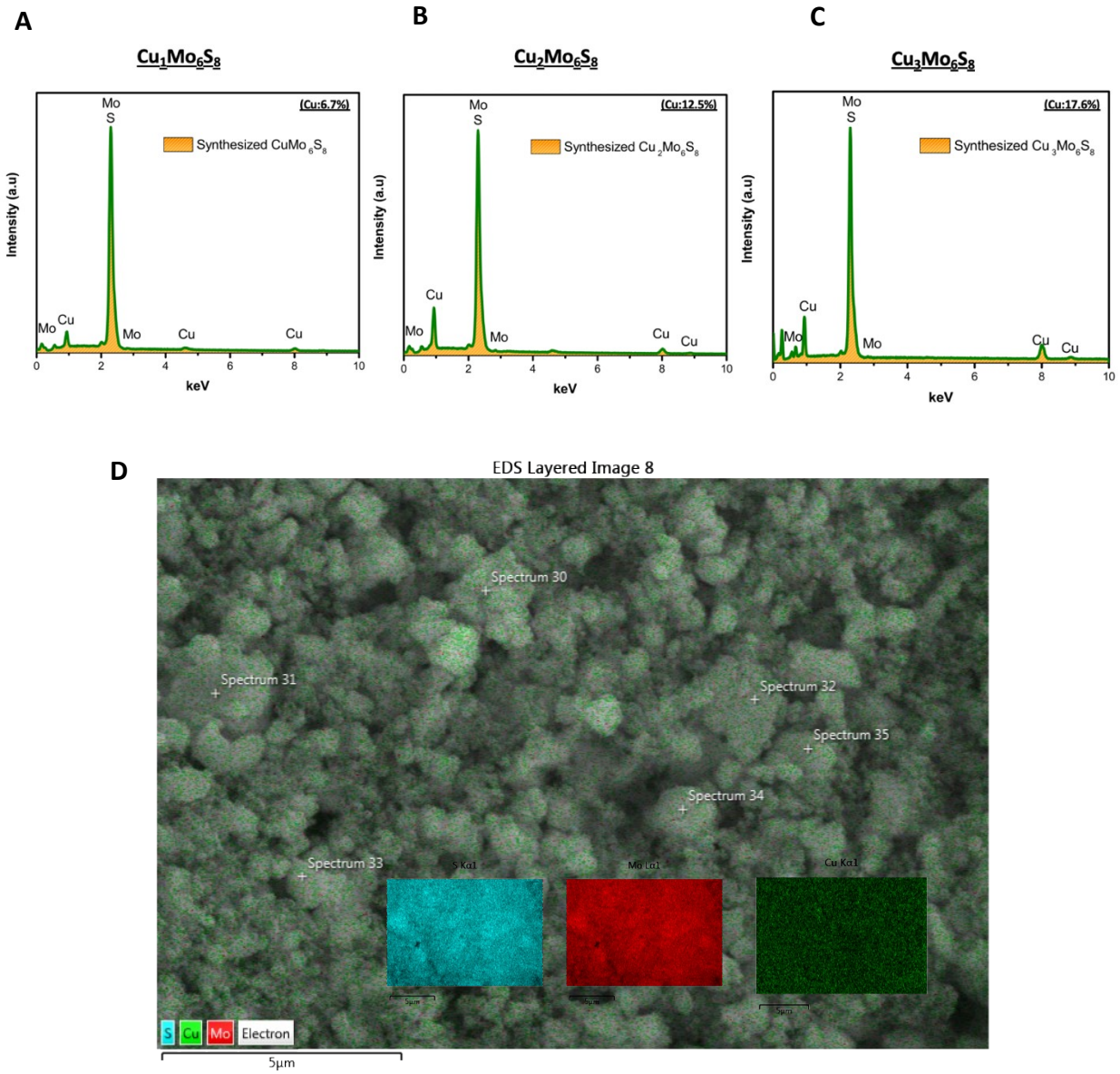

Figure S7. EDX of (A) $Cu_1Mo_6S_8$, (B) $Cu_2Mo_6S_8$, (C) $Cu_3Mo_6S_8$ with their accompanying atomic precents of copper agreeing well with the stoichiometric phase. (D) A representative elemental map scan showing uniform distribution of Cu throughout the experimental samples.

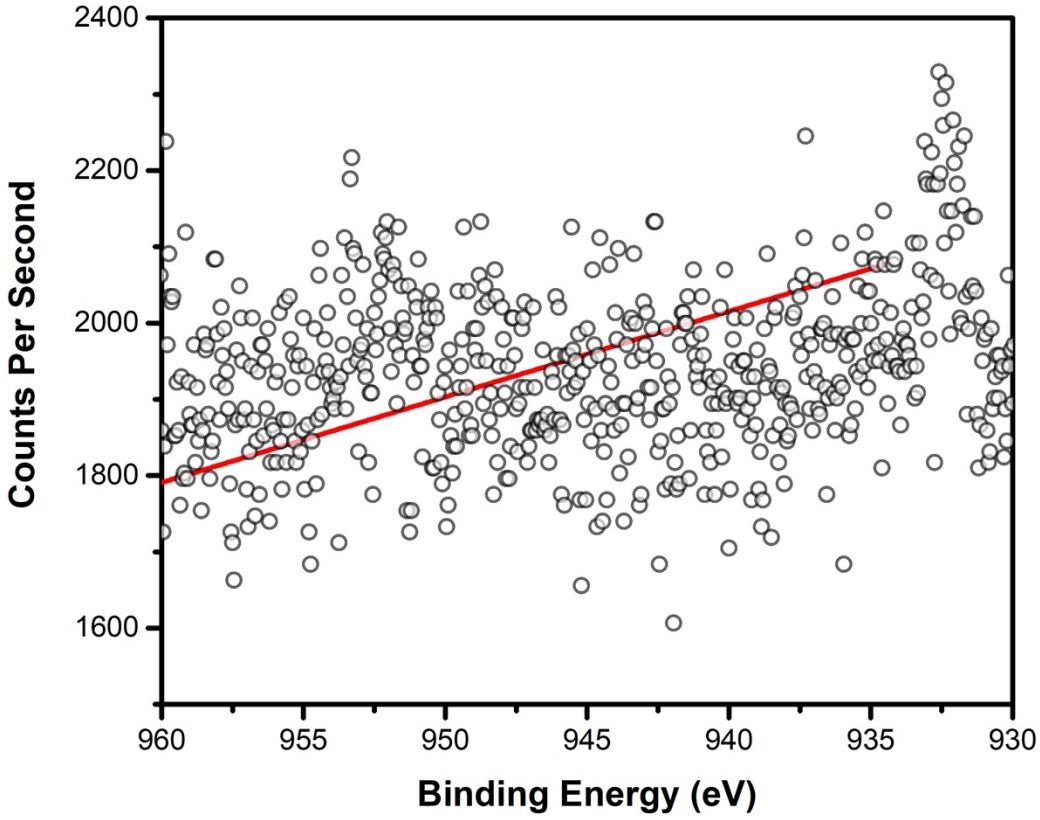

Figure S8. Cu 2p XPS binding region, showing absence of metal in the starting Mo_6S_8 binary phase.

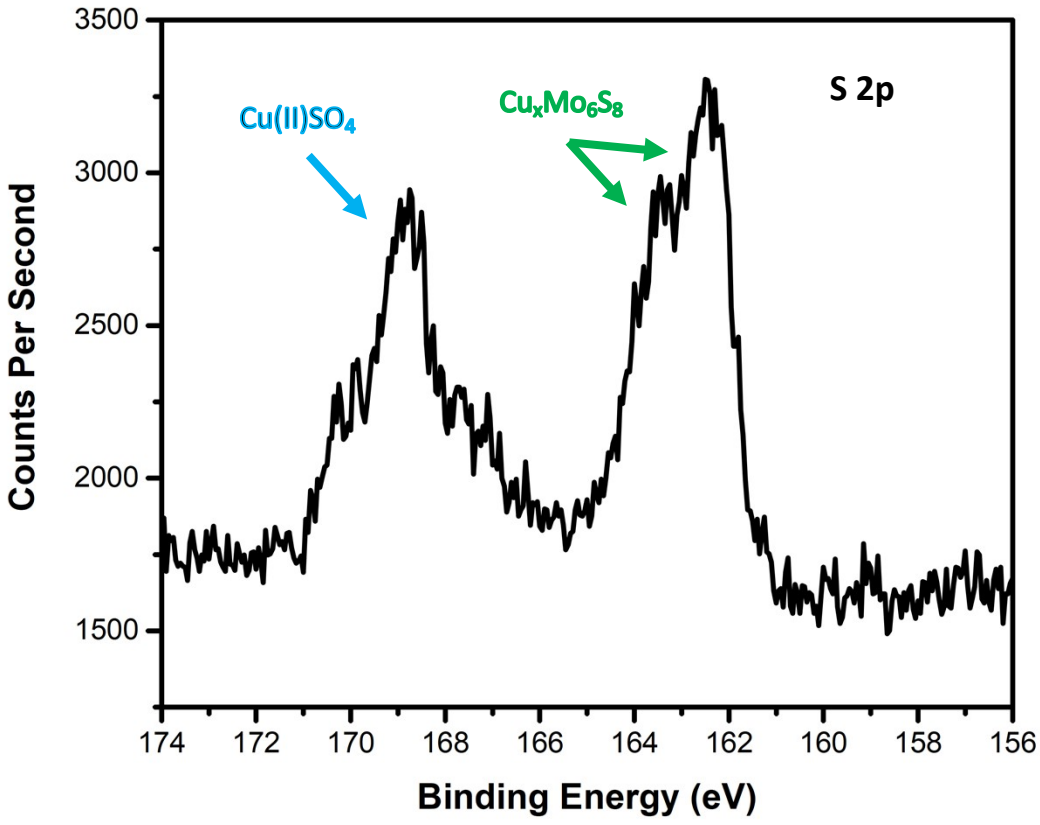

Figure S9. S 2p XPS spectra showing the presence of residual SO_4^{2-} electrolyte at 169 eV. Arrows are to guide the eye to $CuSO_4$ (blue) and the CP (green) contributions to the S 2p signal, respectively.

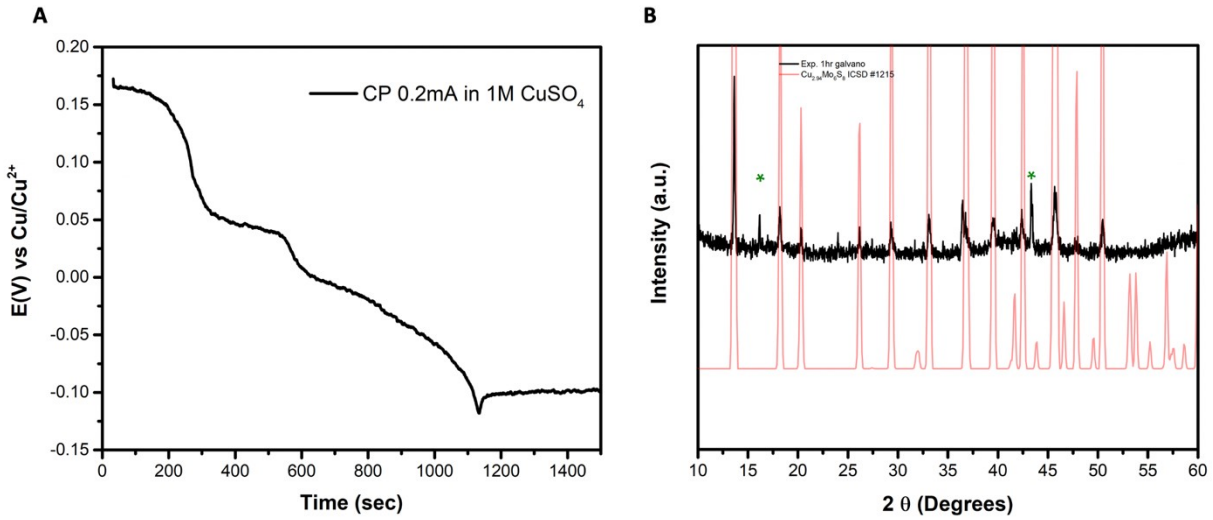

Figure S10. (A) Galvanostatic intercalation experiment in 1M $CuSO_4$, Cu metal reference and counter electrodes, and current density 0.2 mA cm^{-2}. (B) Experimental ex-situ PXRD data of the galvanostatic experiment. Green asterisk in (B) denotes unidentified peaks in the experimental PXRD.

References

[1] Marbán Salgado, J. A.; Uruchurtu Chavarín, J.; Mayorga Cruz, D. Observation of Copper Corrosion Oxide Products Reduction in Metallic Samples by Means of Digital Image Correlation, *Int. J. Electrochem. Sci.* **2012**, 7, 1107 - 1117